

Magnetic and related properties of Tb_4Sb_3 compound

T.I.Ivanova^{1,4}, S.A.Nikitin¹, A.V.Morozkin², G.A..Tskhadadze¹, J.Mulak³,
A.Pikul³, Wojciech Suski^{3,4,a}, D.Badurski³, K.Wochowski³

¹ Physics Department of Moscow State University, Vorobiovy Gory, Moscow 119992, Russia

² Chemistry Department of Moscow State University, Vorobiovy Gory, Moscow 119992, Russia

³ Polish Academy of Sciences, W.Trzebiatowski Institute of Low Temperature and Structure
Research, P.O.Box 1410, 50-950 Wrocław 2, Poland

⁴ International Laboratory of High Magnetic Fields and Low Temperatures, P.O.Box 4714, 50-985
Wrocław 47, Poland

^a corresponding author, e-mail address: w.suski@int.pan.wroc.pl

Keywords: 75.20.En; 75.30.Kz; 75.30.Vn; 72.15.-v; 72.20.My; 64.70.Kb;

Abstract. An X-ray phase analysis and the metallographic examination were employed in the investigation of crystal structure of the Tb_4Sb_3 compound. Magnetic properties have been studied by means of magnetometric measurements, including a magnetocaloric effect, electrical resistivity and magnetoresistivity, and specific heat in broad temperature and the magnetic field ranges on a polycrystalline sample. It was confirmed that the Tb_4Sb_3 compound is an antiferromagnet with the temperature of the magnetic transition, $T_N = 111.4$ K (specific heat) or 114 K (magnetization). The results are discussed in the term of a crystal field splitting scheme.

Introduction.

The Sb containing intermetallic compounds have been found to exhibit interesting physical properties, such as e.g. $PrOs_4Sb_{12}$ [1]. However, among the anti- Th_3P_4 - type compounds of rare earths only those which exhibit the mixed valence state (Eu,Sm,Yb) have been intensively investigated (for review see Ref.[2]).

The anti- Th_3P_4 - type compounds of rare earth elements crystallize in cubic symmetry with space group (s.g) $I\bar{4}3d$ in which there is one distinct Tb and one distinct Sb site. The Tb site is at the position 16(c) with one free coordinate, x , and the Sb site 12(a) with no free coordinates. Generally, the rare earth ions (R) can be thought of as lying on the $1-d$ chains, running parallel to the four body diagonals. In the case of the compounds with the ions exhibiting the mixed valence state, it gives the charge separation e.g of the Yb^{2+} and Yb^{3+} ions (see e.g. [3]). The R ions are coordinated octahedrally by the pnictogen ions. However, there is some indication that this coordination polyhedron may be distorted. The R ions lying on the body diagonal ($[111]$ direction) are equally spaced and can be viewed as forming the chain. The other ions form three chains in the $[1\bar{1}1]$, $[11\bar{1}]$ and $[\bar{1}11]$ directions where the atoms in chains are equivalent.

The antimonides of the light lanthanides appeared to exhibit the same cubic crystal structure anti- Th_3P_4 -type [2]. The Ce_4Sb_3 compound turned out to exhibit ground state ferromagnetic properties with possible Kondo interaction [4,5]. Neutron diffraction showed, however, a commensurate antiferromagnetic structure for this compound in zero magnetic field [6] and a metamagnetic transition in large applied fields. Gd_4Sb_3 shows a second order ferromagnetic transition at $T_C \sim 260$ K and does not exhibit any other transition [7]. The magnetic and thermal

properties of the isostructural $\text{Gd}_4(\text{Sb,Bi})_3$ are given in [8], where the magnetocaloric effect derived from the temperature and magnetic field dependences of the magnetization is presented for this compound. It is to be noted that although the antimonide and bismuthide seem to be close to each other the isostructural Tb_4Bi_3 is ferromagnetic below about 200 K [9]. But the reason could be that the magnetic measurements were carried out in relatively high magnetic field. Recently, the magnetic ordering of the Ln_4Sb_3 compounds, where $\text{Ln} = \text{Pr, Nd, Sm}$, and of $\text{Pr}_2\text{Nd}_2\text{Sb}_3$ was examined by magnetic measurements and neutron diffraction (ND) [10]. Sm_4Sb_3 is a ferromagnet below $T_C = 168$ K. ND study revealed many magnetic transitions for the remaining compounds (for details see [10]).

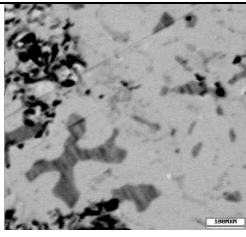
Recently, the structure, magnetic properties in moderated magnetic fields and magnetic structure of Tb_4Sb_3 have been investigated [11]. These experiments have shown that the Tb_4Sb_3 is antiferromagnetic below 108 K in zero magnetic field whereas in fields above ~ 0.3 T a metamagnetic transition to a ferromagnetic state is observed. Neutron diffraction experiment in zero applied magnetic field shows that below the Néel point, $T_N = 112(4)$ K, this compound exhibits an antiferromagnetic flat spiral-type ordering with the propagation vector $\mathbf{K}_1 = [\pm 1/8, \pm 1/8, \pm 1/8]$. The magnetic moment of the Tb atoms is found to be $M_{\text{Tb}} = 6.7(3) \mu_B$ at 80 K. The magnetic moments of the Tb atoms lie in the (111) plane of the Tb_4Sb_3 unit cell (the cone axis arranges along the [111] direction with a cone angle $\beta = 90^\circ$). Below $T_{N2} \sim 50$ K the antimonide shows the second antiferromagnetic transition with $\mathbf{K}_2 = [1/2, 1/2, 1/2]$ with a possible reorientation of Tb magnetic moments. The spin reorientation transition arises presumably from the competition between magnetic exchange and crystalline electric field.

In this paper we present the results of more careful structural analysis, magnetic and magnetocaloric data, the electrical resistivity, magnetoresistivity and specific heat of Tb_4Sb_3 measured in broad temperature and magnetic field ranges on a polycrystalline sample.

Experimental details

Technology and crystal structure. The investigated alloy was obtained as it was described before in Ref.11, in an electrical arc furnace under argon atmosphere using non-consumable tungsten electrode and water-cooled copper tray. Zirconium was used as a getter in the melting process. The alloys were remelted twice in order to achieve complete fusion and homogenous composition. The obtained alloys were annealed at 1170 K for 200 h in a evacuated quartz ampoule containing zirconium chips as a getter and then was quenched by dropping the ampoule into ice-cold water. The structure of the compound was studied using X-ray phase analysis and metallography. The X-ray diffraction was performed on a diffractometer DRON-3.0 – type (Cu K_α radiation, $2\Theta = 20$ -70 deg, step 0.05 deg, 2 sec per point). The obtained diffractograms were identified and evaluated using the *Rietan*-program [13] in the isotropic approximation. A „Neophot” microscope was employed for the metallography ($\times 250$, $\times 500$). The results of this procedure are shown in Table 1. One can see that the product is almost single-phased and contains except of the main Tb_4Sb_3 phase (85%) (anti- Th_3P_4 – type) also two other phases: TbSb (11%) and Tb_5Sb_3 (4%). Note that this contamination is not unique for our sample, because it was reported that in Nd_4Sb_3 the refinement discovered the 1:1 impurity phase NdSb as the second crystallographic phase amounting to 17% [10]. Moreover, recently Zeng et al. [12] found that the α Dy_4Sb_3 is not stable at 500°C. The possible impact of these impurities on the obtained results will be discussed below.

Table 1. Composition of terbium antimonide sample.

Alloys (sample code)	SEM Photo	Mass fraction	Phase	Structure	a, nm	c, nm	X_R	X_{Sb}
Tb ₄ Sb ₃ (BS43B) Arc-furnace melting + annealing at 1170 K for a 200 h in argon. Quenching in ice-cold water		0.85	Tb ₄ Sb ₃	Th3P4	0.91518(7)		0.5712(3)	
		0.11	TbSb	NaCl	0.6179(1)			
		0.04	Tb ₅ Sb ₃	Mn ₅ Si ₃	0.8925(6)	0.6217(5)	0.255(7)	0.639(7)

Physical measurements. Magnetic properties were examined in magnetic fields up to 50 kOe in the temperature range $T = 1.9 - 400$ K using a commercial Quantum Design SQUID magnetometer. The magnetocaloric effect (MCE) was measured by direct method a certain stable temperature. The current through the magnet was switched with aid of a high speed electronic rectifying arrangement and was established the necessary value of magnetic field during 3 s. Then the value of ΔT -effect was measured and magnetic field was smoothly reduced. We had possibility to reach magnetic field up to 13.4 kOe. Electrical resistivity and magnetoresistivity were measured using a home-made equipment at temperatures from 4.2 to 300 K. A Quantum Design PPMS platform was used to measure specific heat between 2 – 300 K in magnetic fields 0 - 5 T.

Results and discussion

The magnetization (M) vs. magnetic field for Tb₄Sb₃ at 1.9 K is presented in Fig.1. One can see that the saturation magnetization amounts to about 32 μ_B /f.u. at magnetic field of 50 kOe which corresponds to about $\sim 7.5 \mu_B$ per Tb atom. The $M(H)$ plot taken in very low magnetic fields is almost linear (Fig.1) and this may suggest that we are dealing with a metamagnetic transition in critical fields of about 4 – 5 kOe. This result is in close agreement with that presented in Ref.11.

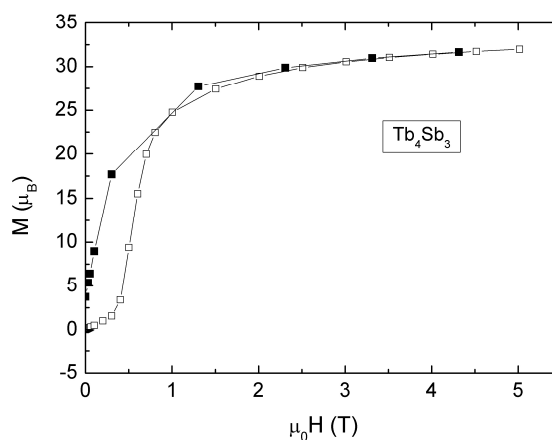


Fig.1. Magnetization versus magnetic field at 1.9 K.

This is confirmed in Fig.2 which demonstrates the magnetization vs. temperature measured in low magnetic field of 50 Oe and in 50 kOe. In this Figure the maximum in $\sigma(T)$, corresponding to Néel point, is clearly seen. The absolute value of the magnetization increases as the magnetic field

increases but the temperature of the maximum (114 K) is not too sensitive to the applied magnetic field (not shown). The smooth $\sigma(T)$ curves taken at low temperatures and presented in Fig.2 prove that the admixture of TbSb in the sample is not meaningful because this compound is antiferromagnetic below $T_N = 14.2$ K with a magnetic moment of $M_{\text{eff}} = 8.2 \mu_B$ [14] and the Fig. does not show any magnetic anomaly at this temperature. There is also no indication of spin reorientation transition reported in Ref.11, either. There is a small difference in the zero field cooled (ZFC) and field cooled (FC) plots. However, the curve obtained in a magnetic field of 50 kOe is typical of a ferromagnet. Moreover, the $\sigma(T)$ curve exhibits a distinct peak which persists in both plots obtained in the ZFC and FC runs. Results of Fig. are also in good accord with those presented in Fig.2a of Ref.11 showing the real part of ac magnetization. The temperature dependence of dc magnetization of Ref.11 shows additional anomaly at 20 K which is absent in our experiment. The reason for this discrepancy seems to be in different magnetic field applied in both experiments.

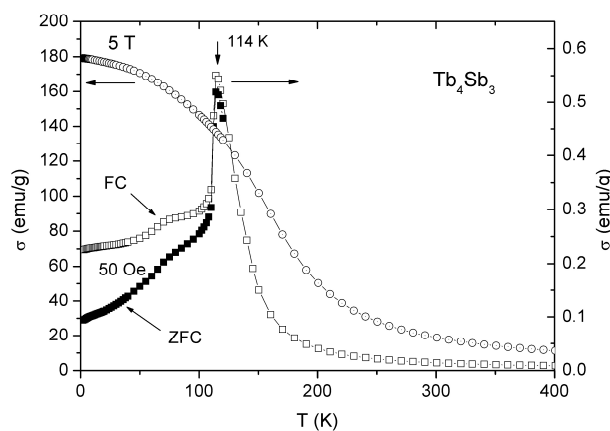


Fig.2. Magnetization, σ , versus temperature measured in magnetic field of 50 Oe in the zero field cooled (ZFC – full symbols) and the field cooled (FC – open symbols) (right hand scale) sample and in 5 T (left hand scale) versus temperature .

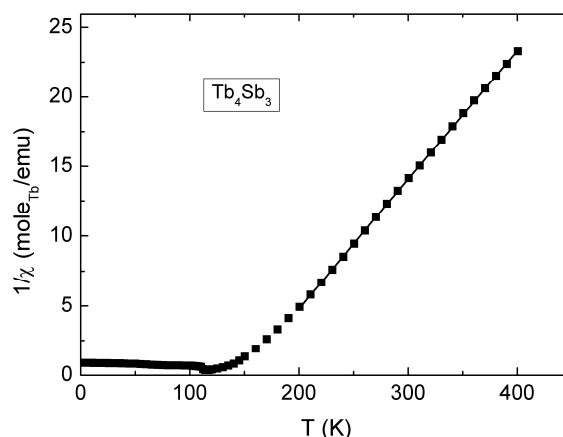


Fig.3. Reciprocal magnetic susceptibility versus temperature measured in magnetic field of 50 Oe. The bold curve is described by the modified Curie – Weiss (MCW) law.

The reciprocal magnetic susceptibility versus temperature measured in magnetic field of 50 Oe is displayed in Fig.3. The magnetic susceptibility follows the modified Curie – Weiss law

(MCW) $\chi = \chi_0 + C(T - \theta)^{-1}$ above about 200 K with the temperature independent magnetic susceptibility χ_0 amounting to -0.001 emu/mol, Curie constant $C = 43.59$ and the paramagnetic Curie temperature $\theta_p = 147$ K. The effective magnetic moment, $p_{\text{eff}} = 9.19 \mu_B$ per terbium atom, is close to the free ion value ($9.72 \mu_B$). Although the ND and low field magnetometric measurements show the antiferromagnetic ordering of Tb_4Sb_3 , the positive paramagnetic Curie temperature seems to indicate predominantly ferromagnetic exchange interactions. We do not believe that the positive θ_p results from the CEF interactions. The susceptibility measurements do show a slight indication of saturation just above T_N which is consistent with the broad Schottky anomaly at about 125 K shown by the heat capacity (see Fig.7).

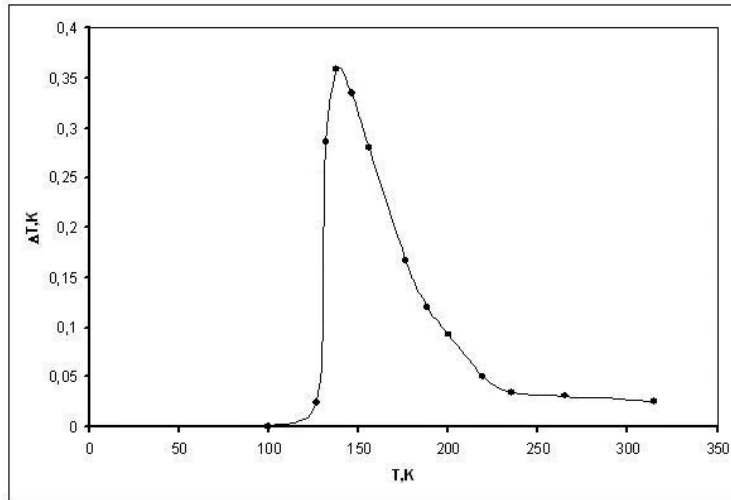


Fig.4. The MCE versus temperature at magnetic field of 13.5 kOe.

The magnetocaloric effect (MCE) is presented in Fig.4. It is known that the MCE has maximum magnitude in the area of the magnetic phase transition. At present we cannot decide if the observed anomalies in $M(T)$ or in $C_p(T)$ correspond to first or second order phase transitions. The maxima seen in Figs.2 and 7 are rather sharp but no thermal hysteresis is observed in these plots.

A maximum in the MCE is observed near the Curie point at $T = 126$ K for $\Delta H = 13.5$ kOe, where $\Delta T = 0.37$ K. This value is not a surprise because recently Zverev et al. [15] on the basis of theoretical consideration have estimated the upper bound of the adiabatic temperature change $\Delta T \ll 18$ K. We also try to get the quantitative estimation of the MCE resulting from paraprocess using the following formula:

$$\Delta T_{\text{ad}} = -\frac{T}{C_H} \int_0^H \left(\frac{\partial M}{\partial T} \right)_H dH, \quad (1)$$

where C_H - a heat capacity in $H = 50$ kOe and about T_C (Fig.7), M - a value of magnetization in the field after achievement by the sample of the assumed one domain structure (Fig.1). Using $H=50$ kOe and $C_H = 200$ J/molK, the value of ΔT was estimated to be about 2.25 K.

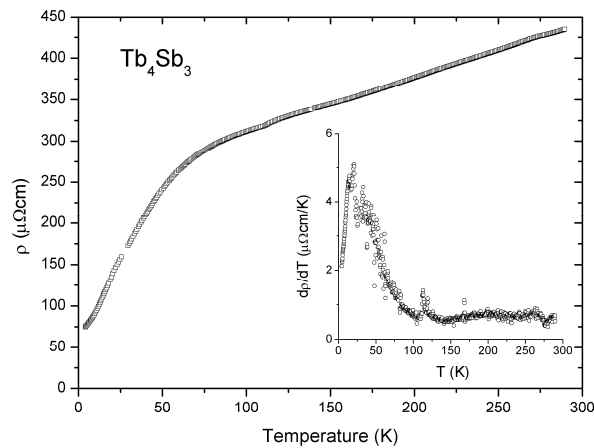


Fig.5. The electrical resistivity versus temperature. Inset shows the $d\rho/dT$ versus temperature plot.

Electrical resistivity versus temperature is shown in Fig.5. The plot is typical for metals, with $RRR \sim 5.9$ but the Néel point could be determined only from the $d\rho/dT$ versus T curve (inset of Fig.5). Although, there is only a local maximum at about 120 K and the temperature of the absolute maximum could correspond to the Néel point of the terbium monoantimonide or to low temperature magnetic phase transition (spin reorientation) reported in Ref.11, but at present we cannot give a final conclusion.

In Fig.6 the magnetoresistivity (MR), $\Delta\rho/\rho_0$ versus magnetic field is presented. In the upper inset the temperature dependence of MR is shown. One can see that MR is negative and typical for field induced ferromagnetism. The magnetic field of 8 T shifts the critical point to 200 K where the $\Delta\rho/\rho_0$ curve reaches 0. The curves $\Delta\rho/\rho_0$ vs. $\mu_0 H$ are reciprocal to the magnetization curves for the typical ferromagnet, where the saturation magnetizations decreases with the increase of temperature. Upper inset shows MR vs. temperature in magnetic field of 8 T. Full squares demonstrate the reciprocal magnetization. The details of the low field MR at low temperature, where spin reorientation transition is observed, are shown in the lower inset.

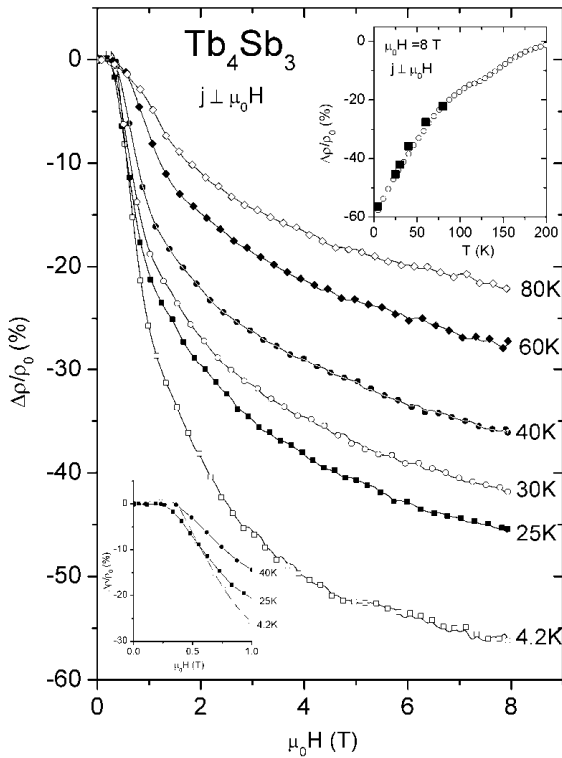


Fig.6. Magnetoresistivity, $\Delta\rho/\rho_0$ versus magnetic field for various temperatures. Upper inset shows MR vs. temperature in magnetic field of 8 T. Full squares demonstrate the reciprocal magnetization. The details of the low field MR at low temperature where metamagnetic transition is observed, are shown in the lower inset.

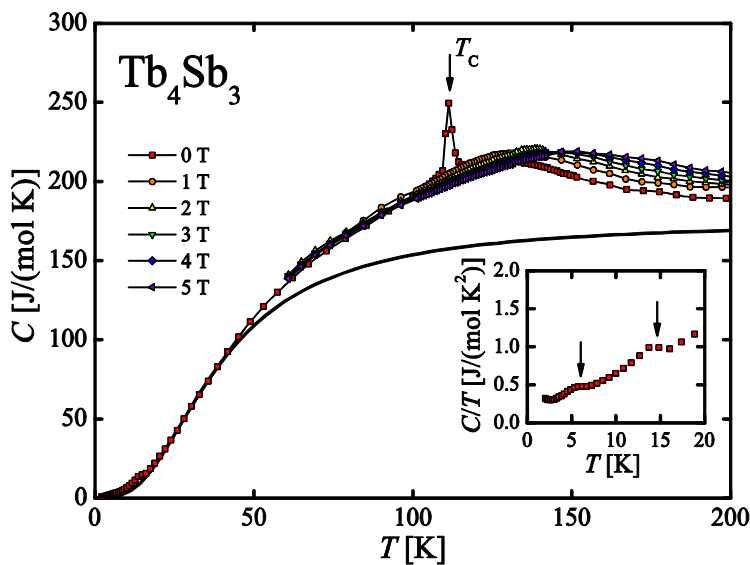


Fig.7. Specific heat versus temperature measured in magnetic field of 0 - 5 T. Inset shows C/T vs. T plot at low temperature.

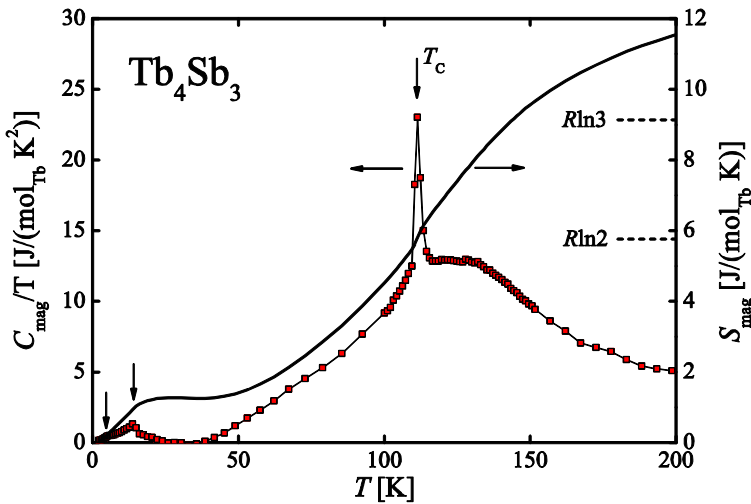


Fig.8. The magnetic entropy (right hand scale) and magnetic specific heat over temperature (left hand scale) versus temperature.

The specific heat against temperature plot measured in magnetic field 0 – 5 T is shown in Fig.7. One can see, the λ – type anomaly is clearly observed at $T = 111.4$ K, the temperature very close to that determined in other experiments where it was considered as the Néel point.. This maximum is suppressed already in a field of 1 T and this behavior corresponds to that presented in Fig.2. There is another diffuse maximum at 130.9 K which is a broad Schottky anomaly. The magnetic field shifts this anomaly to higher temperatures. The inset shows the C/T vs. T dependence at low temperature, yielding the coefficient of the electronic specific heat, $\gamma = 75$ mJ/(mol K²). The solid line corresponds to an estimation of the phonon contributions obtained by the conventional Debye formula adapted for a 7-atoms particle with as low Debye temperature as possible.

There are the additional anomalies at low temperature in inset at temperature corresponding roughly to T_N of TbSb or to low temperature phase transition of Tb₄Sb₃ reported in Ref.11. At present we are not able to confirm these suppositions. An interesting observation is that the magnetic field has much stronger impact on the specific heat above T_N than below, however it is expected for an induced moment system, where the magnetic entropy may be quite small at the ordering temperature. Fig.8 shows the temperature dependence of the magnetic entropy and the magnetic specific heat obtained by the subtraction of estimated phonon contribution (see Fig.7) from the total (measured) specific heat over temperature in the broad temperature range. One can see that both Néel temperature and the Schottky anomaly are more pronounced than in $C(T)$ plot (Fig.7). The magnetic entropy shows an anomaly at low temperature which can correspond to beginning of population of the first excited level. Then the magnetic entropy increases moderately amounting to $R \ln 2$ indicating importance of the doublet. Generally, the entropy is quite small compared to the expected $R \ln 3$ value for Tb³⁺, indicating the presence of strong crystalline electric field splitting. At T_N the clear anomaly in $S(T)$ dependence is missing, indicating that the magnetic

phase transition does not change the CEF level scheme.

Conclusion

The proximity of TbSb and Tb₅Sb₃ phases in the Tb – Sb phase diagram makes it difficult to isolate the latter as a pure phase. The magnetic impurities found by resistivity and specific heat measurements probably originate from neighboring phases. However, a careful analysis and the combination of three different techniques allowed to infer the intrinsic magnetic behavior of Tb₄Sb₃.

As found in this study, the magnetic ordering of the metamagnetic type in Tb₄Sb₃ is due to the localized 4*f* electrons. However, the consideration of the crystal structure mentioned above, which is cubic, but forms a low symmetry coordination polyhedra around the Tb ion, allows following conclusion. As the consequence, the degeneracy of the CEF levels of the 4*f*⁹ electrons of the Tb³⁺ ion is totally lifted and the scheme of the crystal field levels is composed from singlets or pseudo-doublets. This conclusion is clearly indirect. Therefore, the magnetic ordering has an induced character. The easy saturation results from the close separation of the ground and the first excited CEF states in relation to the strong magnetic exchange interactions (relatively high Néel point). Magnetoresistivity is typical for ferromagnetic materials, in spite of the fact that the ferromagnetic order has an induced character.

Determined magnetocaloric effect is low and has no practical meaning, however one should note that was determined in relatively low magnetic field.

The results of thermodynamic examination confirms the importance of the crystal field interaction. At present we do not know why the coefficient of electronic specific heat is relatively enhanced; one of possibilities is presence of a secondary phase. The location of the λ -type anomaly confirms nicely the temperature of magnetic phase transition found in other experiments.

For further understanding of the physical properties of the Tb₄Sb₃ compound, more sophisticated experiments on the single crystal sample are indispensable. It would be very interesting to confirm our assumption about crystal field by inelastic neutron scattering.

Acknowledgment

This work was supported by RFBR Grant 10-02-00721a and RFBR Grant 10-02-90016 Bela. The authors are grateful to Professor R. Troć for scientific discussion. We would like to express our gratitude to R.Gorzelnia, M.Sc. for SQUID measurements.

References

- [1] E.D.Bauer, N.A.Frederick, P.C.Ho, V.S.Zapf, M.N.Maple, *Phys.Rev.* **B65** (2002) 100506.
- [2] T.Palewski, W.Suski in: *Landolt-Börnstein Numerical Data and Functional Relationships in Science and Technology*, New Series, Group III:Condensed Matter, Vol.27subvol.B3, ed.H.P.J.Wijn, Springer Verlag, Berlin 2000, pp.1-361.
- [3] U.Staub, M.Shi, C.Schulze – Briese, B.D.Patterson,, F.Fauth, E.Dooryhee, L.Sonderholm, J.O.Cross, D.Monnix, A.Ochiai, *Phys.Rev.***B71** (2005) 075115.
- [4] A.Ochiai, Y.Nakayabashi, Y.S.Kwon, K.Takeuchi, K.Takegara, S.Suzuki, T.Kasuya, *J.Magn.Magn.Mater.* **52** (1985) 304 .
- [5] T.Suzuki, O.Nakamura, N.Tomonaga, S.Ozeku, Y.S.Kwon, A.Ochiai, T.Takeda, T.Kasuya, *Physica* **B163** (1990) 131.
- [6] R.Nirmala, A.V.Morozkin, O.Isnard, A.K.Nigam, *J.Magn.Magn.Mater.* **321** (2009) 188.
- [7] F.Holtzberg, T.R.McGuire, S.Methfessel, J.C.Suits, *J.Appl.Phys.***35** (1964) 1033.
- [8] X.K.Niu, K.A.Gschneidner,Jr., A.O.Pecharsky, V.K.Pecharsky, *J.Magn.Magn.Mater.* **234**(2001) 193.
- [9] M.Drzyzga, J.Szade, J.Deniszczyk, J.Michalewski, *J.Phys.:Condens.Matter* **15** (2003) 3701.
- [10] C.Ritter, A.V.Morozkin, K.S.Oskolkov, R.Nirmala, O.Isnard, P.Manfrinetti, A.Provino, *J.Alloys Comp.* **494** (2010) 28.
- [11] A.V.Morozkin, R.Nirmala, A.K.Nigam, *J.Alloys Comp.* **450** (2008) 131.
- [12] L.Zeng, J.He, J.Jan, W.He, *J.Alloys Comp.* **479** (2009) 173.
- [13] Fujio Izumi, *RIGAKU J.*, **6(1)** (1989) 10.
- [14] Y.Nakanishi, T.Sakon, M.Motokawa, M.Ozawa, T.Suzuki, M.Yoshizawa, *Phys.Rev.*,**B68** (2003) 1444227.
- [15] V. I. Zverev, A. M. Tsihin, M. D. Kuzmin, *J. Appl. Phys.* **107** (2010) 043907.

Solid Compounds of Transition Elements

doi:10.4028/www.scientific.net/SSP.170

Magnetic and Related Properties of Tb₄Sb₃ Compound

doi:10.4028/www.scientific.net/SSP.170.60